# Pushing down the contrast: the scientific performances of the SPHERE IFS

R. Claudi[1a], J. Antichi[b], A. Baruffolo[a], P.Bruno[c], E.Cascone[d], V.DeCaprio[d], M. DePascale [a], S.Desidera[a], V. D'Orazi[a] , D. Fantinel[a], G. Farisato[a], E. Giro[a], R. Gratton[a], L. Lessio[a], A.L. Maire[e], D. Mesa[a], B. Salasnich[a], , S. Scuderi[c] , E. Sissa[a], M. Turatto[a], A. Zurlo[a,h,l,m], JL Beuzit [f], A. Boccaletti[g], G. Chauvin[f], K. Dohlen[h], G. Finger[i] , J.H. Girard[i], M. Kasper [i], N. Hubin [i], M. Langlois[j], J.L. Lizon[i], D. Mouillet[f], P. Puget [f], F. Wildi[k],

[a] INAF, Astronomical Observatory of Padova, vicolo Osservatorio, 5 35122 Padova Italy
[b] INAF, Astrophysical Observatory of Arcetri, Florence Italy
[c]INAF, Astrophysical Observatory of Catania, via S. Sofia, 78, 95123, Catania Italy
[d] INAF, Astronomical Observatory of Napoli,Salita Moiariello, 16, 80131 - Napoli
[e] Max-Planck-Institut für Astronomie, Königstuhl 17, 69117, Heidelberg, Germany
[f] Institut de Planétologie et d'Astrophysique de Grenoble, B.P. 53, F-38041 Grenoble Cedex 9, France
[g] Observatoire de Paris - section Meudon LESIA, 5 place Jules Janssen, 92195 Meudon
[h] Laboratoire d'Astrophysique de Marseille, B.P. 8, F-13376 Marseille Cedex 12, France
[i] ESO,European Southern Observatory (ESO), Karl-Schwarzschild-Str.2, 85748 Garching,Germany
[j] Centre de Recherche Astrophysique de Lyon (CRAL)
[k] Observatoire de Geneva, Sauverny, CH-1290 Versoix, Suisse
[l]Núcleo de Astronomía, Facultad de Ingeniería, Universidad Diego Portales, Av. Ejercito 441, Santiago, Chile
[m]Departamento de Astronomía, Universidad de Chile, Casilla 36-D, Santiago, Chile
[n]Dipartimento di Fisica e Astronomia, Università degli studi di Padova, Italy

## ABSTRACT

The VLT second generation instrument SPHERE (Spectro-Polarimetric High-contrast Exoplanets Research) was commissioned in the Summer of 2014, and offered to the community in the Spring of 2015. SPHERE is a high contrast imager that exploits its three scientific channels in order to observe and discover young warm exoplanets in the glare of their host stars. The three scientific instrument are: ZIMPOL, a polarization analyzer and imager that works in the visible range of wavelength, IRDIS a dual band imager and spectro polarimetric Camera that works in the NIR range up to K band, and IFS, an integral field spectrograph working in the YJH band. Very important is the complementarity between IRDIS and IFS. The former has a larger Field of view (about 12 arcseconds) while the IFS push its examination very close to the central star (FoV ~ 1.7 arcsec). In one year of operational time a lot of very interesting scientific cases were investigated and very nice results were gathered. In this paper we would like to focus the attention on the high quality results and performances obtained with the IFS

**Keywords:** Instrumentation, Extrasolar Planets, High Contrast Imaging, Integral Field Spectrograph

## 1. INTRODUCTION

The search for extrasolar planets is still dominated by radial velocity and transit methods. The latter with Kepler satellite[1] and the foreseen transit missions (CHEOPS[2], PLATO[3], TESS[4]) discovered and will discover thousands of new worlds. In spite of this, big efforts have been done in order to direct imaging these low mass companions. In the last two – three years a number of high contrast imagers were commissioned at 8 – 10 m class telescopes among which Gemini Planet Imager (GPI) and SPHERE. The Gemini Planet Imager saw its first light at the Gemini South telescope in November 2013 and achieved H-band Strehl ratios of ~0.9 and 5σ contrasts of $10^5$—$10^6$ at separations of 0.35-0.75"[5]. Data analyses of commissioning observations of β Pictoris b[8] and HD 95086 b[(6,7,8)] were published[(5,9)]. SPHERE was commissioned in

[1] riccardo.claudi@oapd.inaf.it, tel.. +39 0498293499

Ground-based and Airborne Instrumentation for Astronomy VI, edited by Christopher J. Evans, Luc Simard, Hideki Takami
Proc. of SPIE Vol. 9908, 99083H · © 2016 SPIE · CCC code: 0277-786X/16/$18 · doi: 10.1117/12.2232827

the Summer of 2014 and offered to the community in the Spring 2015. In this paper a brief overview of SPHERE and of the IFS is given along with some of the first scientific results.

## 2. SPHERE AND IFS OVERVIEW

SPHERE (see Figure 1) consists of four subsystems: the Common Path Optics and three science channels, the differential imaging camera (IRDIS)[10], the Integral Field Spectrograph (IFS)[11], and the visible imaging polarimeter (ZIMPOL)[12]. The Common Path includes pupil stabilizing fore optics (tip-tilt and derotator), the SAXO[13] extreme adaptive optics system with a visible wavefront sensor, and NIR coronagraphic devices in order to feed IRDIS and IFS with highly stable coronagraphic images.

The IRDIS science module covers spectral range from 0.95-2.32 microns with an image scale of 12.25 mas consistent with Nyquist sampling at 950 nm. The FOV is 11″ × 12.5″, both for direct and dual imaging. Dual band imaging is the main mode of IRDIS, providing images in two neighboring spectral channels with < 10 nm rms differential aberrations. Two parallel images are projected onto the same 2k × 2k detector with 18-micron square pixels, of which they occupy about half the available area. A series of filter couples is defined corresponding to different spectral features in modeled exoplanet spectra. The classical imaging mode allows high-resolution coronagraphic imaging of the circumstellar environment through broad-, medium-, and narrow-band filters throughout the NIR bands including Ks. In addition to these modes, long-slit spectroscopy at resolving powers of 50 and 500 is provided, as well as dual polarimetric imaging mode. A pupil-imaging mode for system diagnosis is also implemented.

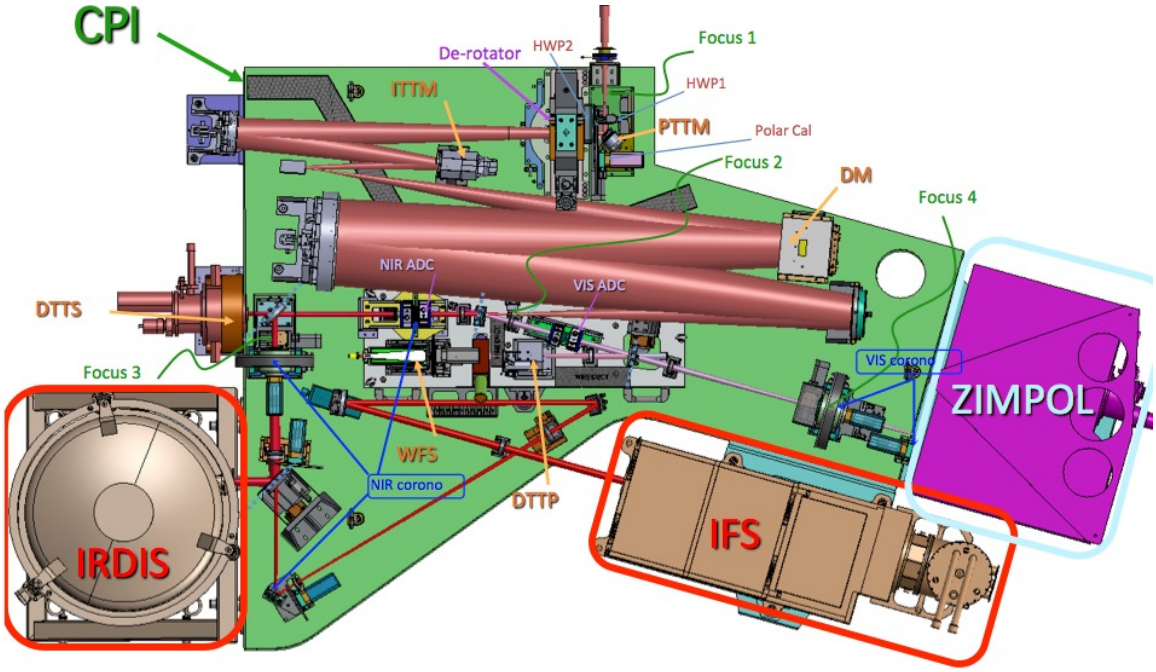


Figure 1: Overview of the inner part of SPHERE. The optical path that feeds the Common path and the three scientific instruments is clearly shown.

ZIMPOL is located behind the SPHERE visible coronagraph. The working bandwidth ranges between 600-900 nm with instantaneous field of view of 3″ x 3″ with access to a total field of view of 8″ in diameter via an internal field selector. The ZIMPOL optical train contains a common optical path that is split by a polarizing beamsplitter in two optical arms, each with its own detector. The common path contains common components for both arms like calibration components, filters, a rotable half wave plate and a ferroelectric liquid crystal polarization modulator. The two arms have the ability to measure simultaneously the two complementary polarization states in the same or in distinct filters. The images on both ZIMPOL detectors are Nyquist sampled at 600 nm. The basic ZIMPOL principle for high-precision polarization measurements includes a fast polarization modulator with a modulation frequency in the kHz range, combined with an

imaging photometer that demodulates the intensity signal in synchronism with the polarization modulation. The polarization modulator and the associated polarizer convert the degree-of-polarization signal into a fractional modulation of the intensity signal, which is measured in a demodulating detector system by a differential intensity measurement between the two modulator states. Each active pixel measures both the high and low states of the intensity modulation and dividing the differential signal by the average signal eliminates essentially all gain changes, notably changes of atmospheric transparency or electronic gain drifts.

IFS explores the stellar neighborhood in order to find planetary spectral features. This quest is conducted searching for strong $CH_4$ absorption bands in both the stellar light reflected by gaseous Jupiter-like planets and in thermal emission from young-warm planets. The IFS is also designed to provide first order characterization of the low mass companion itself. Additional science topics addressed by SPHERE include the study of protoplanetary discs, brown dwarfs, evolved massive stars and Solar System and extragalactic science. The heart of IFS[11] is a new kind of lens-based IFU called BIGRE[14]. BIGRE is built as a double face lenselet array in which the second lenslet array allows formation of pseudo-slit images corresponding to very small portions of the field, which are then imaged on the detector after being dispersed. The array is made by 150 × 150 lenslets with 161.5 μm pitch allowing a total FoV of 1.77" × 1.77". Specifically, BIGRE is placed at the interface of the IFS with the Common Path (CP) and it is optically conjugated with the telescope Focal Plane, that is re-imaged by an F/# = 316 beam. This allows to sample the diffractive PSF - arising from the AO compensation and the Coronagraphic spatial filtering, both working inside the CP optics - at the Nyquist's limit.

The purpose of the IFS is thus to realize diffraction limit Integral Field Spectroscopy with the high contrast capabilities of BIGRE. To this scope, the whole IFS system, which lays downstream the entrance lenslet array, only re-images and disperses these slits with the highest optical stability and a good optical quality. The optimized IFS optical design is a fully dioptric, made by several optics located along a straight optical axis. The IFS is designed to work at different resolutions in two different wavelength ranges: R~50 in the 0.95 -1.35 μm (z-J mode) and R~30 in the wider wavelength range of 0.95 – 1.65 μm (z-J-H mode). The two resolutions are achieved by two different Amici prisms while the working wavelength ranges are defined by a combination of band pass, high- and low-pass filters mounted inside the dewar (low pass filter) and just in front of the prisms (band pass filter for the z-J mode and high pass filter for the z-J-H mode). The spectrograph is not cryogenic so a set of filters and baffles are used to minimize the thermal background noise. Most of the unwanted radiation is eliminated by the presence of a cold filter, about 40 mm before the detector and by two baffles, a cold absorbing baffle located inside the dewar, and a warm reflecting baffle located on the back of the IFS camera. The residual thermal background is mainly due to unavoidable thermal emission from the active IFS optical components.

IFS is mostly used together with IRDIS in the so-called NIRSUR (NIR survey) mode, developed for the large survey that uses about 80% of the GTO time. It combines IRDIS dual imaging in H band with imaging spectroscopy using the IFS in the Y-J bands (IRDIFS mode). This configuration permits to benefit simultaneously from the optimal capacities of both dual imaging over a large field (out to ~5" radius) and spectral imaging in the inner region (out to at least 0.7" radius). In particular, it allows to reduce the number of false alarms and to confirm potential detections obtained in one channel by data from the other channel. This will be a definite advantage in case of detections very close to the limits of the system. Other possible observing modes are IFS in Y-J-H band simultaneously with IRDIS in Ks band and IFS in Y-J simultaneously with IRDIS in H broad band.

## 3. COMMISSIONING TEST AND RESULTS

During commissioning of SPHERE (hereafter called COM1 and COM2) the following test has been performed to characterize the instrument:

- Photometry and Flux Calibration;
- Astrometry
- High Contrast performances Validation

### 3.1 Photometric Accuracy of faint companions using flux calibration

SPHERE IRDIFS data are usually normalized using the flux calibration. The latter was used to evaluate photometry for a number of faint companions by considering the contrast at 1.25 and 1.65 micron. We called these magnitudes J_IFS and H_IFS. The Table 1 summarizes the results from commissioning sky tests[22,23,24] and compares them with literature values.

On the whole, there is good agreement. There is one discrepant case (J magnitude for HD1160 B[23]); however, our photometry yields J-H=0.47, that is much better in agreement with expectations for such a late M-star than the value of J-H=1.18 given in the discovery paper by Nielsen et al.[15]. Also, the result from the Y-J observation of HR8799d[22,24] is of very poor quality, and should not be considered. Once these cases are eliminated, the standard deviations of the derived magnitudes with respect to literature values are 0.06 mag for Y_IFS, and 0.17 mag for H_IFS.

Table 1: Results of Photometry of faint companions using flux calibration (see text).

| Star | Sep. | Star | | Literature | | Contrast | | Measured | | Offset | |
|---|---|---|---|---|---|---|---|---|---|---|---|
| | arcsec | J | H | J | H | ΔJ | ΔH | J_IFS | H_IFS | ΔJ | ΔH |
| Y-J | | | | | | | | | | | |
| HD223816 B | 0.57 | 8.92 | 8.69 | 14.6 | | 4.72 | | 14.64 | | 0.04 | |
| REJ1925-366 B | 0.22 | 9.31 | 8.97 | 14.6 | | 5.25 | | 14.56 | | -0.04 | |
| PZ Tel b | 0.36 | 6.86 | 6.49 | 12.26 | 11.87 | 5.43 | | 12.29 | | 0.03 | |
| HIP102790 B | 0.63 | 2.15 | 1.38 | | | 8.28 | | 10.43 | | | |
| HR7581 B | 0.25 | 2.29 | 1.65 | | | 8.34 | | 10.63 | | | |
| HD114714 B | 0.64 | 5.61 | 5.31 | 16.06 | | 10.40 | | 16.01 | | -0.05 | |
| HR8799 d | 0.63 | 5.38 | 5.28 | 18.24 | 17.21 | 13.3: | | 18.68: | | 0.43: | |
| Y-H | | | | | | | | | | | |
| PZ Tel B | 0.36 | 6.86 | 6.49 | 12.26 | 11.87 | 5.31 | 5.37 | 12.17 | 11.86 | -0.09 | -0.01 |
| REJ1925-366 B | 0.22 | 9.31 | 8.97 | 14.6 | 14.6 | 5.33 | 5.97 | 14.64 | 14.94 | 0.04 | 0.34 |
| HD1160 B | 0.77 | 6.98 | 7.01 | 15.83 | 14.65 | 8.18 | 7.68 | 15.16 | 14.69 | -0.67 | 0.04 |
| Gamma Sgr B | 0.20 | 1.26 | 0.77 | | | 8.29 | 8.43 | 9.55 | 9.20 | | |
| HR7581 B | 0.25 | 2.29 | 1.65 | | | 8.48 | 8.78 | 10.77 | 10.43 | | |
| HR8799 d | 0.63 | 5.38 | 5.28 | 18.24 | 17.21 | 12.96 | 11.83 | 18.32 | 17.11 | 0.08 | -0.10 |
| HR8799 e | 0.40 | 5.38 | 5.28 | | 16.86 | 12.74 | 11.70 | 18.12 | 16.98 | | |

### 3.2 Astrometry

During commissioning various astrometric fields were observed, in both field and pupil stabilized modes[16]. The calibration for IFS data has been obtained by the analysis of the IRDIS data (in particular the H2 images) and using the transformation of IFS to IRDIS coordinates provided by the internal distortion grid. The resulting scale for IFS is 7.45± 0.01 mas/pixel[23, 25].

### 3.3 High Contrast performances Validation

In order to obtain an estimate of the contrast performance of the IFS, several deep coronagraphic observations in pupil stabilized mode with the Apodized Lyot Coronagraph (ALC) have been obtained.

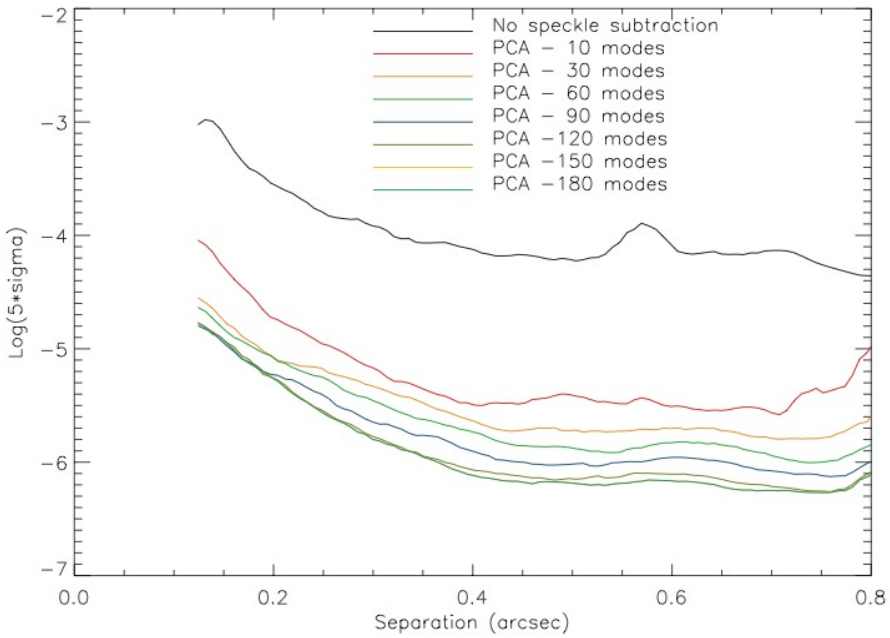


Figure 2: 5-sigma contrast curves from Y-J image of HR7581 obtained using PCA-based differential imaging. The curves were corrected for cancellation effects using fake planets.

Figure 2 gives the 5-sigma contrast as a function of separation of the faint companion from the central star. Results are given for Principal Component Analysis (PCA)[17] done with different number of modes. Cancellation effects are considered using corrections estimated from fake planets. The noise model indicates that this observation is calibration limited. The limiting contrast is -6.19 ($6.5\times10^{-7}$) at 0.5 arcsec and almost flat for separation >0.4 arcsec. The contrast depends also by the rotation angle of the field during the overall acquisition. This dependence was determined using only fractions of the total exposure for two bright objects (HR7581 and Altair). The plot shown in **Error! Reference source not found.Error! Reference source not found.**Figure 3**.** gives the contrast as a function of time.

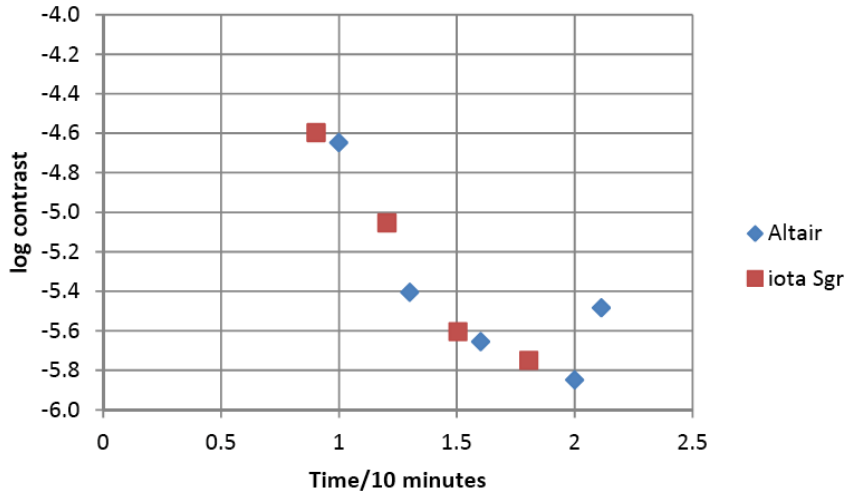


Figure 3: Trend of the contrast with angle/time (see text)

The same measurements have been performed with the different coronagraphs available for the IFS. In order to perform these, the bright star α Hyi (HR591, J=2.30) was observed with different coronagraphs. The Figure 4 shows the 5-sigma contrast curves without any differential imaging applied for the Y-J case. Results at separation smaller than the Inner Working Angle (IWA) of 0.10 arcsec (0.12 arcsec) were not considered for ALC2 (ALC3). As expected, best contrast is

obtained with APO2 (the smoothest apodizer) and ALC3 (the mask with the largest occultation). 4Q performs slightly worse than the apodized Lyot coro's. For a review of these type of coronagraph see Guyon et al.[18].

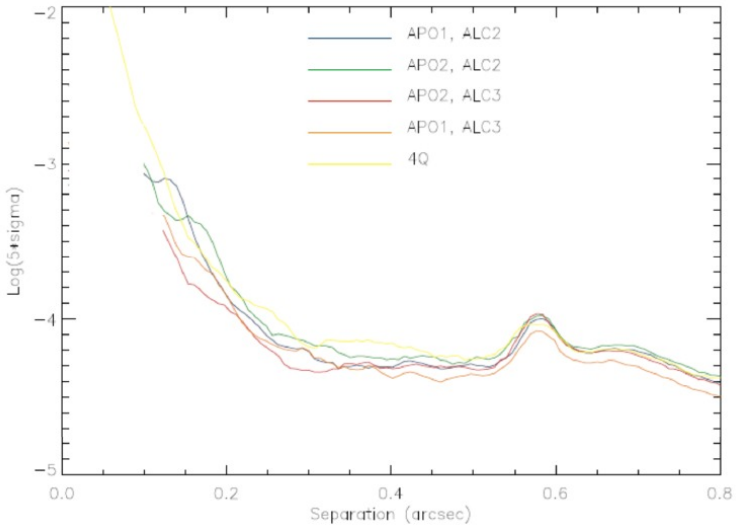


Figure 4: Contrast curves for different coronagraphs available for IFS.

All measurements have been performed also for Y-H mode of IFS. Performance in Y-H mode are similar to those obtained for the Y-J ones.

## 4. SCIENCE WITH IFS

IFS allowed to obtain a contrast better than $10^{-6}$ at a separation of few tenths of arcsec. One example is the contrast plot obtained for Sirius displayed in Figure 5. The contrast was obtained applying at the same time both Angular Differential Imaging (ADI[16]) and Spectral Differential Imaging (SDA[19,20]) exploiting the principal components analysis (PCA[17]) algorithm adapted to the SPHERE IFS case[21], this is only for IFS and the reduction is made in an independent way from those that is shown in Vigan et al.[25].

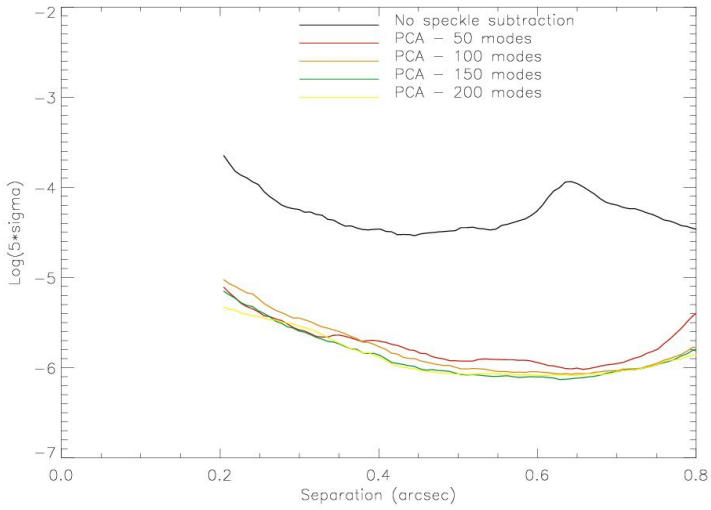


Figure 5 - Contrast plot for Sirius obtained with different number of principal components for the PCA

This contrast allow to find companion even at small separations from the host star like for the case of HR3549 B[28] that is shown in Figure 6 where the companion is clearly visible at edge of the instrument field of view (FOV) (separation of

~0.8 arcsec from the host star). In this case the contrast is only ~4 magnitudes in J band so that the companion is in this case a M type star. In Figure 7 we display the low resolution spectrum obtained using the IFS+IRDIS data. Moreover, we superimpose the three spectra taken from two different spectral library: the Montreal Brown Dwarf and Exoplanet Library[2] and the library from Allers & Liu[27]. The best fit is with a L0 star (DENISPJ104731.1-181558[27]).

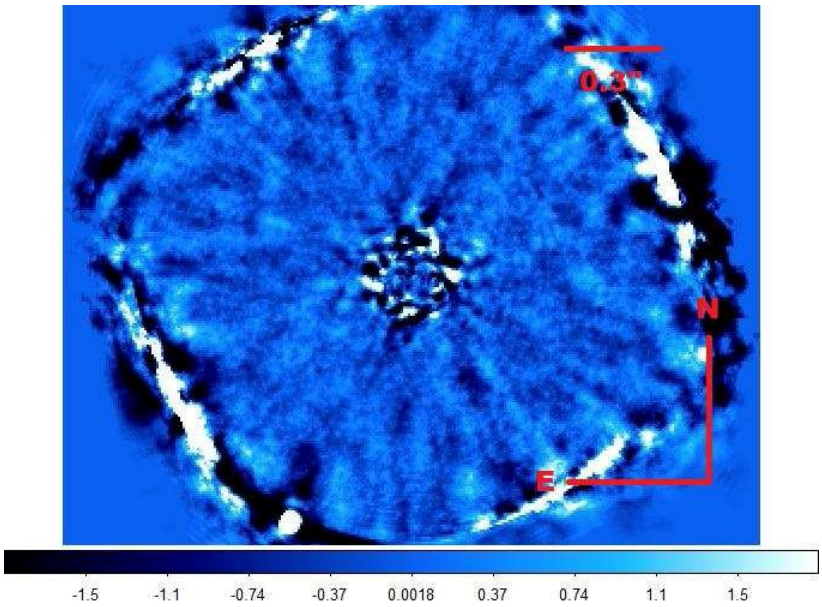


Figure 6 – Final image obtained for HR3549 with IFS

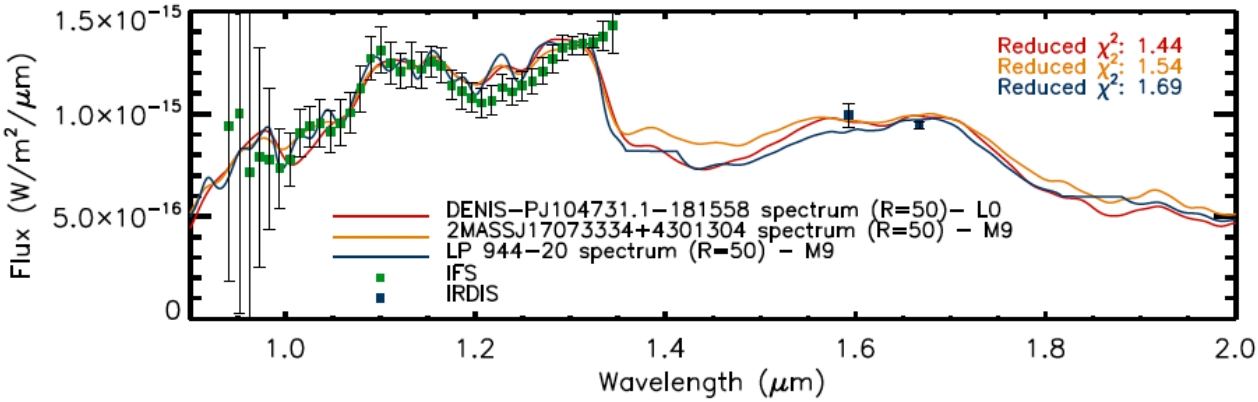


Figure 7 – Low resolution spectrum obtained from the IFS+IRDIS data reduction is displayed with green squares. The error bars for each spectrum value are displayed as well. In different colors we plot the three spectra with a best fit from the spectral libraries described in the text.

To be able to obtain good results for companion with a larger contrast with respect to the host star we need to go at larger separations like for the case of HR 8799. This well studied system is composed by 4 substellar companions and two of them are well into the small FOV of IFS. It was observed during the commissioning of SPHERE[22] and in Figure 8 we display the final image obtained. The two innermost planets are visible at the unprecedented S/N of ~20. Moreover, for both of them it was possible to obtain very good quality spectra like it is shown in Figure 9 for HR8799d and in Figure 10 for HR8799e.

[2] https://jgagneastro.wordpress.com/the-montreal-spectral-library/

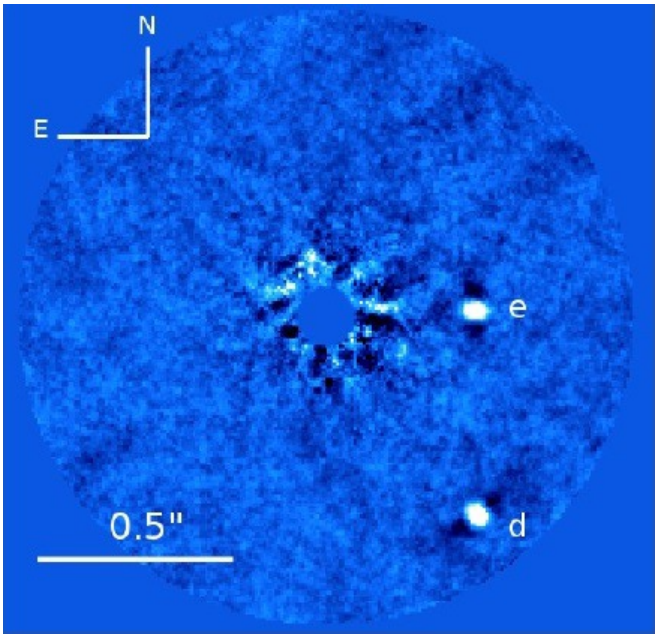


Figure 8 – Final image of the inner part of the HR 8799 system where the two innermost planets are clearly visible

Both in Figure 9 and in Figure 10 together with the lower resolution spectrum from IFS we inserted the photometric points from IRDIS (blue dots) that can allow enlarging the spectral range. Moreover, some spectra of known objects are inserted in the plot so that a spectral classification is possible trying the spectrum the better fir the extracted one. In this way, it has been possible to define that the best fit for both the planet was a L6 spectrum.

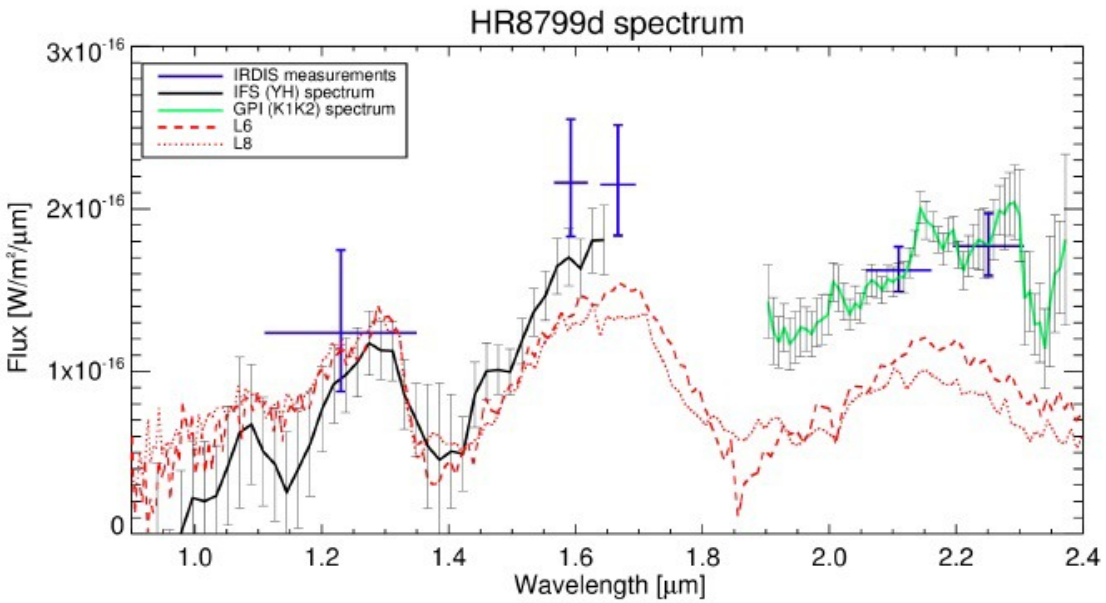


Figure 9 – Extracted spectrum for HR8799d

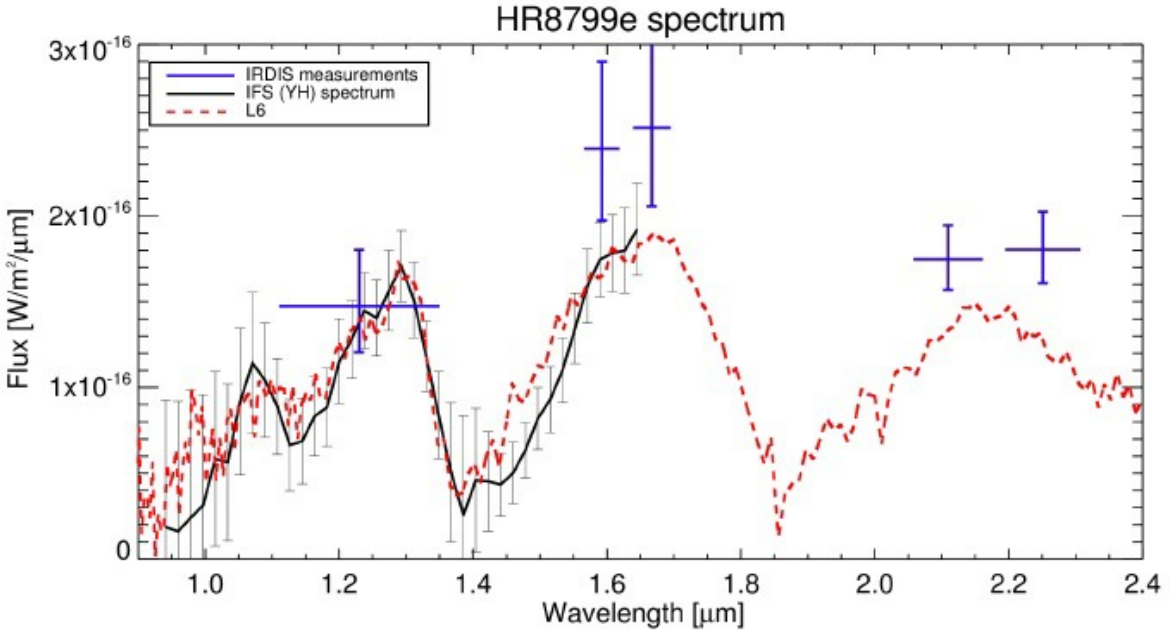


Figure 10 – Extracted spectrum for HR8799e

SPHERE IFS is also being used for detection and characterization of faint circumstellar disks, exploiting the spectral capabilities to explore the wavelength dependence of disk features. In Figure 11 the disk of HD106906AB[29] is shown.

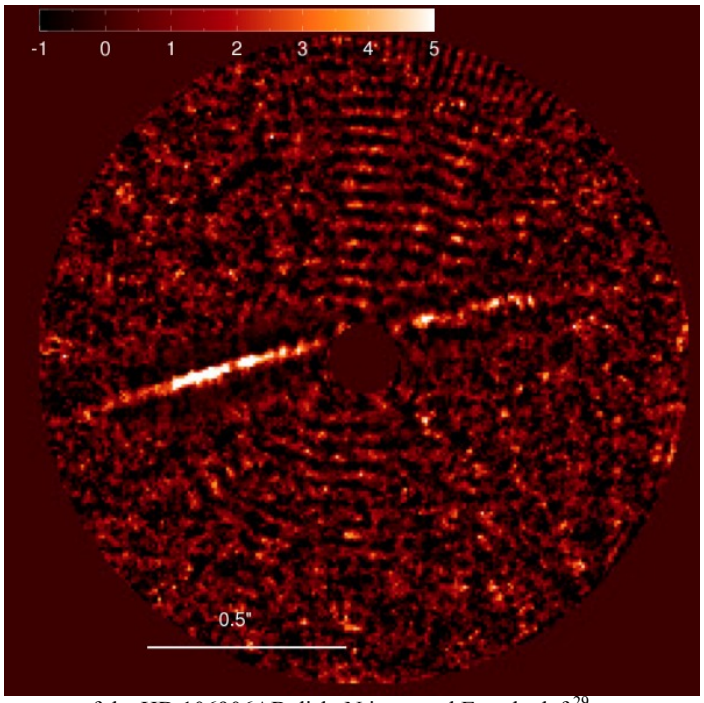


Figure 11: IFS YJH snr map of the HD 106906AB disk. N is up and E to the left[29].

## 5. CONCLUSIONS

SPHERE and its IFS are in action since 2014 and up to now several interesting results have been obtained. We summarized some of them in this paper. The main thing is that in so far the instrument is working in a fully compliant way with the science requirements stated at the beginning of the project. SPHERE is and will be one of the new generation instrumentation that allow the characterization of giant planets and brown dwarfs orbiting young stars opening a new frontier in the search and physical characterization of young and warm planets and small mass companion.

## REFERENCES


[1] Borucki W.J., KEPLER Mission: development and overview, Rep. Prog. Phys., 79, 036901, (2016)

[2] Broeg C.; Benz W.; Fortier A.; Ehrenreich D.; Beck T.; Cessa V.; Alibert Y.; Heng K.; The CHEOPS Mission, American Astronomical Society, ESS Meeting #3, BAAS 47, 6 (2015)

[3] Rauer H. and 151 Authors, The PLATO 2.0 Mission, Exp. Astron., 38, 249, (2014)

[4] Ricker G.R.; Winn J.N.; Vanderspeck R.; Latham D.W.; Bakos G.A.; et al., "Transiting Exoplanet Survey Satellite", J. Astron. Telesc. Instrum. Syst. 1, 014003 (2014).

[5] Macintosh, B., Graham, J.R., Ingraham, P., Konopacky, Q., Marois, C., Perrin, M., Poyneer, L., Bauman, B., Barman, T., Burrows, A., Cardwell, A., Chilcote, J., De Rosa, R.J., Dillon, D., Doyon, R., Dunn, J., Erikson, D., Fitzgerald, M., Gavel, D., Goodsell, S., Hartung, M., Hibon, P., Kalas, P.G., Larkin, J., Maire, J., Marchis, F., Marley, M., McBride, J., Millar-Blanchaer, M., Morzinski, K., Norton, A., Oppenheimer, B.R., Palmer, D., Patience, J., Pueyo, L., Rantakyro, F., Sadakuni, N., Saddlemyer, L., Savransky, D., Serio, A., Soummer, R., Sivaramakrishnan, A., Song, I., Thomas, S., Wallace, J.K., Wiktorowicz, S., Wolff, S., "The Gemini Planet Imager: First Light", PNAS, 111, 12661-12666 (2014)

[6] Rameau, J., Chauvin, G., Lagrange, A.-M., Boccaletti, A., Quanz, S.P., Bonnefoy, M., Girard, J.H., Delorme, P., Desidera, S., Klahr, H., Mordasini, C., Dumas, C., Bonavita, M., "Discovery of a Probable 4-5 Jupiter-mass Exoplanet to HD 95086 by Direct Imaging", ApJL, 772, L15, (2013)

[7] Meshkat, T., Bailey, V., Rameau, J., Bonnefoy, M., Boccaletti, A., Mamajek, E.E., Kenworthy, M., Chauvin, G., Lagrange, A.-M., Su, K.Y.L., Currie, T., "Further Evidence of the Planetary Nature of HD 95086 b from Gemini/NICI H-band Data", ApJL, 775, L40 (2013)

[8] Rameau, J., Chauvin, G., Lagrange, A.-M., Meshkat, T., Boccaletti, A., Quanz, S.P., Currie, T., Mawet, D., Girard, J.H., Bonnefoy, M., Kenworthy, M., "Confirmation of the Planet around HD 95086 by Direct Imaging", ApJL, 779, L26, (2013)

[9] Galicher, R., Rameau, J., Bonnefoy, M., Baudino, J.-L., Currie, T., Boccaletti, A., Chauvin, G., Lagrange, A.-M., Marois, C., "Near-infrared detection, characterization of the exoplanet HD 95086 b with the Gemini Planet Imager", A&A, 565, L4, (2014)

[10] Vigan A., Langlois M.P., Dohlen K., Zurlo A., Moutou C.; Costille A.; Gry C., Madec F., Le Mignant D., Gluck L.; Sauvage J.F., "SPHERE/IRDIS: final performance assessment of the dual band imaging and long slit spectroscopy mode", Proc. SPIE 9147, Ground-based and Airborne Instrumentation for Astronomy V, 91474T (2014)

[11] Claudi R.; Giro E.; Turatto M.; Baruffolo A.; Bruno P.; Cascone E.; DeCaprio V.; Desidera S.; Dorn R.; Fantinel D.; Finger G.; Gratton R.; Lessio L.; Lizon J.L.; Maire A.L.; Mesa D.; Salasnich B.; Scuderi S.; Zurlo A.; Dohlen K.; Beuzit J.L.; Mouillet D.; Puget P.; Wildi F.; Hubin N.; Kasper M; The SPHERE IFS at work, Proc. SPIE, 9147, Ground-based and Airborne Instrumentation for Astronomy V, 91471L (2014)

[12] Roelfsema R., Bazzon A., Schmid H.M., Pragt J.H., Gisler D., Dominik C., Baruffolo A.; Beuzit J.-L.; Costille A.; Dohlen K.; Downing M.; Elswijk E.; de Hann M.; Hubin N.; Kasper M.; Keller C.; Lizon J.-L.; Mouillet D.; Pavlov A.; Puget P.; Salasnich B.; Sauvage J.-F.; Wildi F.; "The ZIMPOL high contrast imaging polarimeter for SPHERE: system test results", Proc. SPIE 9147, Ground-based and Airborne Instrumentation for Astronomy V, 91473W (2014)

[13] Petit C., Sauvage J.F., Fusco T., Sevin A., Suarez M.; Costille A.; Vigan A.; Soenke C.; Perret D.; Rochat S.; Baruffolo A., Salasnich B.; Beuzit J.L.; Dohlen K.; Mouillet D.; Puget P.; Wildi F.; Kasper M., Conan J.-M.; Kulcsar C.; Raynaud H.-F.; "SPHERE extreme AO control scheme: final performances assessment and on sky

validation of the first auto tuned LQG band operational system", Proc. SPIE 9148, Adaptive Optics Systems IV, 91480O (2014);
[14] Antichi, J., Dohlen, K., Gratton, R., et al., "BIGRE: A Low Cross-Talk Integral Field Unit Tailored for Extrasolar Planets Imaging Spectroscopy", ApJ, 695, 1042 (2009)
[15] Nielsen et al. , 2012, ApJ, 750, 53
[16] Marois, C., Lafrenière, D., Doyon, R., Macintosh, B., & Nadeau, D. 2006, ApJ, 641, 556
[17] Soummer, R., Pueyo, L., & Larkin, J. 2012, ApJ, 755, L28
[18] Guyon et al., 2006, ApJSuppl, 167,81
[19] Racine R., Walker G.A.H., Nadeau D., Doyon R., Marois C., Speckle noise and the detection of Faint Companions, PASP, 111, 587 (1999).
[20] Marois C., Doyon R., Nadeau D., Racine R., Riopel M., Vallee P., Lafreniere D., TRIDENT: An Infrared Differential Imaging Camera Optimized for the Detection of Methanated Substellar Companions**,** PASP, 117, 745, (2005).
[21] Mesa, D., Gratton, R., Zurlo, A., et al. 2015, A&A, 576, A121□.
[22] Zurlo, A., Vigan, A., Galicher, R., et al. 2016, A&A, 587, A57
[23] □Maire, A.-L.; Bonnefoy, M.; Ginski, C. et al., First Light of the VLT planet finder SPHERE II. the physical properties and the architecture of the young systems PZ Tel and HD1160 revised, A&A, 587, A56, (2016)
[24] Bonnefoy M., Zurlo A., Baudino J.L., et al., First Light of the VLT planet finder SPHERE IV. Physical and Chemical properties of the planets around HR8799, A&A, 587, A58 (2016)
[25] Maire A.L., Langlois M., Lagrange A.M. et al., SPHERE IRDIS and IFS astrometric strategy and calibration, , This Conference, (2016)
[26] Vigan A., Gry C., Salter G. et al., High Contrast imaging of Sirius A with VLT/SPHERE: looking for giant planets down to one astronomical unit., MNRAS, 454, 129 (2015)
[27] Allers, K. N. & Liu, M. C. 2013, ApJ, 772, 79
[28] Mesa D., Vigan A., D'Orazi V. et al., Characterizing HR3549 B using SPHERE, A&A, in publication
[29] Lagrange A.M., Langlois M., Gratton R. et al., A narrow, edge-on disk resolved around HD 106906 with SPHERE, A&A, 586, L8, (2016)